The 4th International Symposium on More Electric Aircraft Technology (MEA 2017)

8–9 November 2017

Design and operating mode analysis of hybrid actuation system based on EHA/SHA

Liu Zidong, Bai Zhiqiang, Xu Shuhan

Beijing Aeronautical Science & Technology Research Institute of COMAC, Beijing, People's Republic of China
E-mail: liuzidong@comac.cc

Published in *The Journal of Engineering*; Received on 10th January 2018; Accepted on 26th January 2018

Abstract: By analysing the structure and working principle of hybrid actuation system (HAS) which consists of a servo-hydraulic actuator (SHA) and an electro-hydrostatic actuator (EHA), the overall mathematical model with dissimilar redundancy conforms is established, which considers various influencing factors, such as air load and attachment stiffness. Furthermore, the mechanism of dynamic force fighting is expounded. In addition, a new control strategy which uses the trajectory generator and weight coefficient theory is proposed to restrain the force fighting. The modelling and simulation analysis between the new control strategy and a conventional proportional–integral–derivative control strategy is carried out as well. Based on the above researches, quantitative analysis is carried out on the procedure of operating mode switching, which is from active/active mode to active/passive mode. The results indicate that the position/velocity trade-off control strategy has a good control performance, and effectively restrains the static force fighting as well as dynamic force fighting. Besides that, it can also shorten the system response time. The HAS can still meet the actuating requirements after the operating mode switches to active/passive mode. The actuator in passive state generates a certain static error by the reason of tracking the position of the control surface.

1 Introduction

As a transitional form of all electric aircraft, all fields of more electric aircraft (MEA) theories have developed by leaps and bounds. On the concept of MEA, the conventional hydraulic components are being progressively replaced by electrically powered ones. In this way, the MEA can save at least one set of central hydraulic power by using the hybrid actuation system (HAS) which consists of the power-by-wire actuators and hydraulic actuation system. Thereby, the dissimilar redundant actuation has large potential to reduce maintenance cost through the way of reducing the system weight. Meanwhile, it also combines the advantages of flexible cable and high reliability. Since several years ago, Airbus has pioneered the use of '2H/2E (2 sets of hydraulic/2 sets of electric)' networks in various types of airplanes, like A380 and A350 [1], in which some actuators are driven electrically. The architecture like this has made the primary flight control system unprecedented in independence and redundancy.

Due to different working principle and physical parameters of actuators in a HAS, the dynamic characteristics between the power-by-wire actuators and servo-hydraulic actuator (SHA) are quite different. When the two kinds of actuators are used to control one surface at the same time, the force fighting between different channels is more obvious to affect tracking characteristic and damage the control surface structure. To solve this problem, the domestic and overseas scholars have carried out some study works. Aiming at the force fighting in the HAS composed of SHA and electro-mechanical actuator (EMA), Cochoy *et al.* [2] balances the force deviation between two channels by adding feedforward filtering. The mechanism of force fighting in the electro-hydrostatic actuator (EHA)/EMA actuation system is discussed systematically in [3–6]. Meanwhile, the corresponding control strategies are proposed in these papers. In [7], the hydraulic cylinder pressure difference is used as an indicator of the actuator output force. Then, average force is compared with the actuator actual force and passed through integrator to give position signal for reducing force fighting. In [8, 9], the model reference adaptive control strategy and self-tuning fuzzy proportional–integral controller strategy are presented, respectively, for dissimilar dual redundant actuation system which is a combination of SHA and EHA.

In the study on force fighting for HAS right now, the static force fighting control strategies are mostly investigated. However, it is difficult to consider the influences of the dynamic parameters such as velocity and acceleration on the force fighting, so that the whole system cannot achieve the best control effect. There is a paucity of study on the operating state of the HAS based on EHA/SHA, especially for the dynamic characteristic of switching transience between the conventional operating modes with external force.

Aiming at the above problems, this paper uses EHA and SHA to establish a HAS. After discussing the structure of this HAS, this paper proposes a new control strategy with trajectory generator and weight coefficient theory to eliminate the force fighting. The validity of this control strategy is verified by simulation and analysis. Finally, based on the above model, the dynamic characteristic of the switch transience between the active/active mode and active/passive mode (A/P mode) is analysed by the method of mathematical simulation as well. All of these provide the theoretical and practical evidence for the engineering application of HAS.

2 HAS modelling

Assuming that all actuators are in normal working conditions, then the bypass valve, safety valve and other hydraulic components are not considered during modelling. Meanwhile, the control surface deflection angle is not large. It is supposed that the actuators are rigidly connected to control surface, thereby the schematic diagram of the HAS is shown in Fig. 1.

The dashed part in Fig. 1 is SHA with the components of servo valve and hydraulic cylinder, in which the inputs are the servo valve voltage U_S and the external force F_S. The piston position X_S is chosen as the output of SHA. The solid box part is EHA, composed of motor, hydraulic pump and actuating cylinder. The inputs of EHA are the applied voltage U_E and the external force F_E, and the output is the piston position X_E. The flight control surface

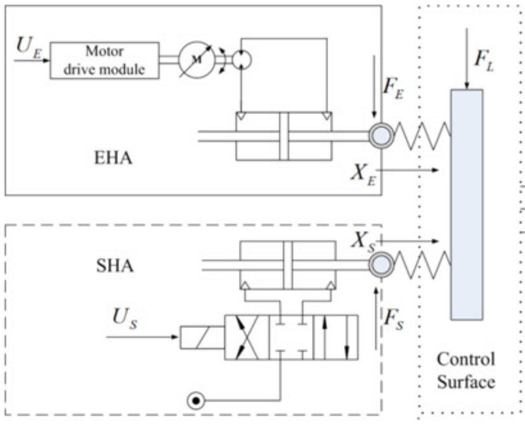

Fig. 1 *Schematic diagram of the HAS*

structure is contained in the dotted part with some certain inputs (X_E, X_S) and outputs (X_L, F_E and F_S).

2.1 Mathematical model of SHA

In order to carry out a qualitative research on the dynamic characteristic of SHA, the non-linearities are ignored in this communication. The basic equations of each module of the SHA system can be obtained as follows.

(i) Voltage balance equation

$$U_S = L_S \frac{dI_S}{dt} + R_S I_S \tag{1}$$

(ii) Spool dynamics equation

$$Q_S = \frac{\omega_S^2 \cdot I_S}{S^2 + 2\xi_S \omega_S s + \omega_S^2} + D_S \Delta P_S \tag{2}$$

(iii) Hydraulic pump pressure equation

$$\Delta P_S = P_{exts} - P_{rets} + P_{losts} \tag{3}$$

(iv) Hydraulic cylinder flow continuity equation

$$\begin{cases} Q_{AS} = D_S \Omega_S = A_S \dfrac{dX_S}{dt} + \dfrac{V_{exts}}{\beta_E} \dfrac{dP_{exts}}{dt} \\ Q_{BS} = -D_S \Omega_S = -A_S \dfrac{dX_S}{dt} + \dfrac{V_{rets}}{\beta_E} \dfrac{dP_{rets}}{dt} \end{cases} \tag{4}$$

(v) Force balance equation

$$A_S P_{exts} - A_S P_{rets} = m_S \frac{d^2 X_S}{dt^2} + B_S \frac{dX_S}{dt} + F_S \tag{5}$$

where R_S is the armature resistance, I_S is the motor current, L_S is the armature inductance, Q_S is the servo valve output flow, ω_S is the servo valve characteristic frequency, ξ_S is the servo valve damping coefficient, D_S is the servo valve flow/pressure gain, ΔP_S is the load pressure difference, P_{exts} is the extension pressure, P_{rets} is the retraction pressure, P_{losts} is the pressure loss, Q_{AS} and Q_{BS} are the output flows of different ports of pump, respectively, A_S is the effective area of hydraulic cylinder piston, m_S is the mass of hydraulic cylinder rod and B_S is the viscous resistance in hydraulic cylinder.

2.2 Mathematical model of EHA

(i) Voltage balance equation

$$U_E = R_E I_E + L_E \frac{dI_E}{dt} + K_E \Omega_E \tag{6}$$

(ii) Torque balance equation

$$K_m I_E = \Delta P_E D_p + J_m \frac{d\Omega_E}{dt} + B_m \frac{d\Omega_E}{dt} \tag{7}$$

(iii) Hydraulic pump pressure equation

$$\begin{cases} P_A = P_{exte} - P_{cde} \\ P_B = P_{rete} - P_{cde} \\ \Delta P_E = P_{exte} - P_{rete} + P_{loste} \end{cases} \tag{8}$$

(iv) Hydraulic cylinder flow continuity equation

$$\begin{cases} Q_{AE} = D_P \Omega_E = A_E \dfrac{dX_E}{dt} + C_{lp}(P_{exte} - P_{rete}) + C_{eq} P_{exte} + \dfrac{V_{exte}}{\beta_E} \dfrac{dP_{exte}}{dt} \\ Q_{BE} = D_P \Omega_E = -A_E \dfrac{dX_E}{dt} + C_{lp}(P_{exte} - P_{rete}) + C_{eq} P_{exte} + \dfrac{V_{exte}}{\beta_E} \dfrac{dP_{exte}}{dt} \end{cases} \tag{9}$$

(v) Force balance equation

$$F_{SE} = A_E P_{exte} - A_E P_{rete} = m_E \frac{d^2 X_E}{dt^2} + B_E \frac{dX_E}{dt} + F_E \tag{10}$$

where R_E describes the armature resistance, I_E is the motor current, L_E is the armature inductance, K_E presents the back EMF constant, Ω_E is angular velocity, K_m is electromagnetic torque constant, D_P is pump displacement, ΔP_E is load pressure difference, J_m is inertia of rotor and coupled shaft, B_m is total damping between motor and coupled shaft, P_A and P_B are the different ports of pump, respectively, Q_{AE} and Q_{BE} are the output flows of different ports of pump, respectively, P_{exte} is the extension pressure, P_{rete} is the retraction pressure, P_{cde} is the accumulator pressure, P_{loste} is the pressure loss, A_E is the effective area of hydraulic cylinder piston, C_{lp} and C_{ip} are the coefficients of the internal and external leakage, β_E is the effective bulk modulus, F_{SE} is the actuating cylinder output force, m_E is the mass of hydraulic cylinder rod and B_E is the viscous resistance in hydraulic cylinder.

2.3 Control surface structure

The control surface structure is modelled to represent the surface inertia, and equal attachment stiffness and damping for the two actuators, then the motion equations of control surface are thus

$$\begin{cases} F_S + F_E = m_L \dfrac{d^2 X_L}{dt^2} + B_L \dfrac{dX_L}{dt} + F_L \\ F_S = K_S(X_S - X_L),\ F_E = K_S(X_E - X_L) \end{cases} \tag{11}$$

where m_L is the mass of hydraulic cylinder rod, B_L is the viscous resistance in hydraulic cylinder and K_S is the transmission stiffness.

When the piston of the actuator extends out of the neutral position, the piston deflects the control surface. Then the aerodynamic load increases with the increase of the deflection angle of the control surface. Assuming that the aerodynamic load and the piston stroke are linear, the equation of air load applied to the actuator can be obtained

$$F_{\mathrm{L}} = \frac{F_{\max} X_{\mathrm{A}}}{X_{\mathrm{A\_max}}} \tag{12}$$

where $F_{\max}$ is the actuator maximum output force, X_{A} is the actuator displacement and $X_{\mathrm{A\_max}}$ is the maximum stroke of actuator.

The structure of the HAS can be obtained from the formula (1)–(12) as shown in Fig. 2.

3 Control strategies for force fighting

The different types of the actuators, because of the inconsistencies of the self-physical characteristics, are not able to output the identical position at any time even under the same position demand, which causes the force fighting to occur. For the HAS studied in this paper, the force fighting between SHA and EHA would be more obvious due to the inherently different dynamic characteristics.

3.1 *Theory analysis on force fighting*

The two channels are both in active state. Based on the analysis of the dynamic force fighting for the EMA/EHA HAS in [3], the equations of the closed-loop system transfer function of each actuator can be obtained by means of analogy.

SHA position transfer function

$$X_{\mathrm{S}} = \frac{X_{\mathrm{C}} - G_2(s)F_{\mathrm{S}}}{G_1(s)} \tag{13}$$

EHA position transfer function

$$X_{\mathrm{E}} = \frac{X_{\mathrm{C}} - H_2(s)F_{\mathrm{E}}}{H_1(s)} \tag{14}$$

where $1/H_1(s)$ and $1/G_1(s)$ describe the position pursuit function of actuators, $G_2(s)/G_1(s)$ and $H_2(s)/H_1(s)$ are the rejection functions of actuators to external force, X_{C} is the position command.

The following equations can be obtained by deduction:

$$\begin{cases} H_{\mathrm{S}} = G_{\mathrm{S}} \\ H_{\mathrm{E}} = G_{\mathrm{E}} - \dfrac{X_{\mathrm{S}} X_{\mathrm{E}}}{X_{\mathrm{S}} + X_{\mathrm{E}}} G_{\mathrm{S}} \end{cases} \tag{15}$$

The formula (15) shows the requirements to eliminate the force fighting of HAS in an ideal condition, which can be described as follows.

(i) The dynamic pursuit performance of each actuator should be identical (the upper equation of formula (15)).
(ii) The dynamic characteristic of against load disturbances of the different actuators should be designed according to the values of their transmission stiffness (the lower equation of formula (15)).

3.2 *Position and velocity trade-off control strategy (control strategy 1)*

In order to eliminate the force fighting of HAS, the primary thing is to ensure that two channels have the similar dynamic characteristic. Therefore, besides the position of the actuator piston, the control strategy should take into account the influence on force fighting caused by expansion speed of the actuator piston. Based on the above principle, this paper comprehensively weighs the impacts of the position and the velocity, and converts them into a control variable by weighting coefficient method.

3.2.1 Mathematical model of trajectory generator: In order to convert position command into reference position and reference velocity, a trajectory generator is constructed by using second-order filter [3]. The schematic diagram is shown in Fig. 3, where ω_i is the reference natural frequency and ξ_i is the reference damping coefficient.

Fig. 3 is an ideal model of the trajectory generator with the selected parameters. In order to meet the control requirements of the HAS, the selected parameters are solved as follows: $\omega_i = 60$ rad/s and $\xi_i = 0.707$.

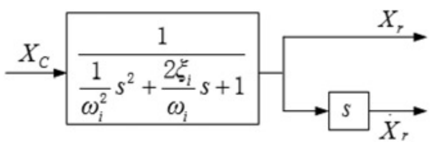

Fig. 3 *Ideal model of the trajectory generator*

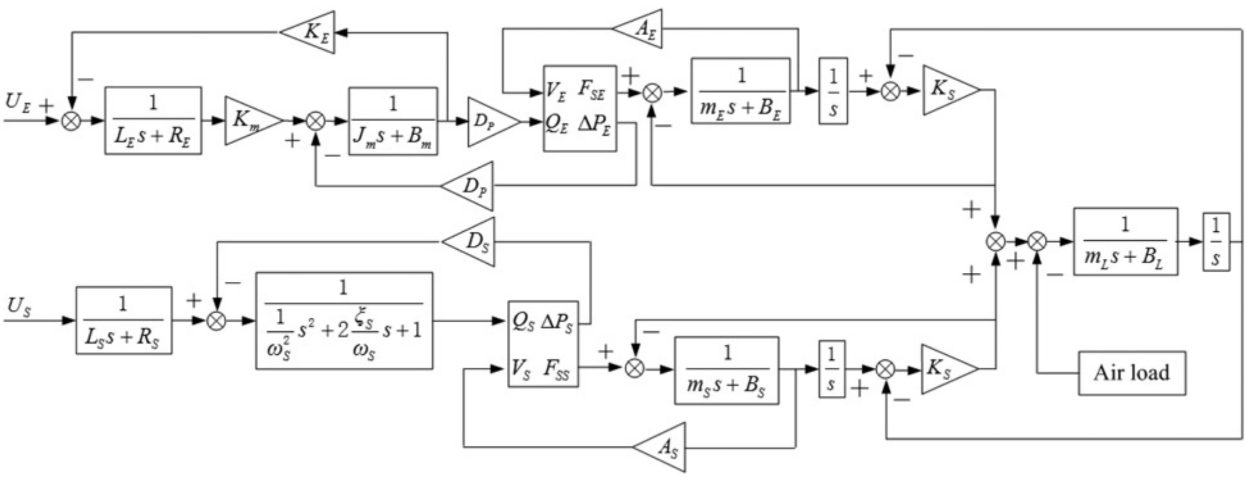

Fig. 2 *Structure of the HAS*

3.2.2 Mathematical model of fitness function: In order to measure the influences of position and velocity of the actuator piston on the entire system synthetically, the concept of fitness function index for the force fighting control strategy is proposed.

First, to shorten the system response time and improve control accuracy, (16) is used to obtain the response measurement index of the system

$$J_X = \int_0^{\infty} t \cdot \Delta X(t)\,\mathrm{d}t \tag{16}$$

Similarly, (17) is chosen as the measurement index to ensure the dynamic characteristic of the system

$$J_v = \int_0^{\infty} t \cdot \Delta V(t)\,\mathrm{d}t \tag{17}$$

Subsequently, this paper uses the weight coefficient method to get fitness function index by comprehensively considering the system response index and dynamic performance index

$$J_f = (1 - \omega_f)J_X + \omega_f J_V \tag{18}$$

where ω_f is weight coefficient.

In this control strategy, the position and the velocity are introduced to compensate the force error between different channels at the same time, thus the whole control model is shown in Fig. 4.

3.3 Force fighting feedback strategy (control strategy 2)

This strategy is widely applied to the similar redundant actuation system, in which the load pressure is an important indicator of the output force on account of the reason that the rest force composed of the jack friction and the inertial force is negligible in comparison with the actuators output force [3]. Then the pressure difference between two channels is used to restrain the force fighting. Following this theory, the force fighting, regarded as the controlled parameter, is used to compensate the position of the actuator after being filtered with proportional–integral–derivative controller. Thereby, the schematic of force fighting feedback strategy is shown in Fig. 5.

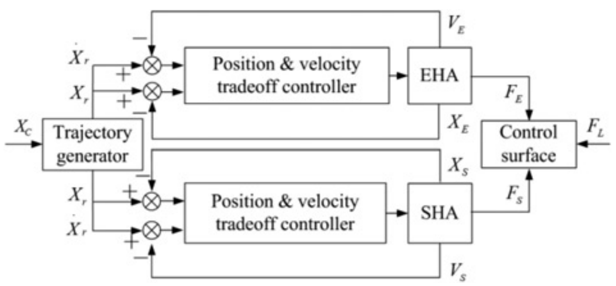

Fig. 4 *Design principle of position/velocity trade-off control strategy*

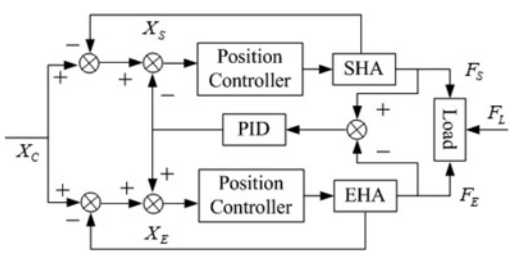

Fig. 5 *Schematic of force fighting feedback strategy*

3.4 Simulation over force fighting

In this section, simulation analysis and comparison are made between the first strategy and the second strategy. The parameters of the actuators are shown in Table 1.

Through simulation, various step disturbances are manually injected at $t = 0$ s, and the simulation results are shown in Figs. 6 and 7.

As described in Fig. 6, all simulations show that all of the control surfaces can reach the instruction position accurately. Besides that, the static force fighting can be retrained obviously under the control of both strategies, respectively. So, the two control strategies can achieve satisfactory control effects on the static force fighting for the HASs.

The control efficiency for the dynamic force fighting of the two controllers can also be seen in Fig. 6. By using the control strategy 1, the response time of the HAS to reach the position command is 0.148 s. Similarly, it spends 0.32 s to reach the value of the instruction position under the control of strategy 2. It means that the control strategy 1 has reduced 2.16 times response time as compared to control strategy 2. This is because the control strategy 2

Table 1 Parameters of both actuators

SHA		EHA	
Parameter	Value	Parameter	Value
L_S, H	0.57	L_E, H	44×10^{-4}
R_S, Ω	100	R_E, Ω	0.13
X_{max}, mm	50	X_{max}, mm	50
A_S, m^2	0.0021	A_E, m^2	0.0046
ω_S, s^{-1}rad	520	M_E, kg	3
ξ_S	0.38	J_m, m^{2}kg	0.002
M_S, kg	2	K_m, m^{2}kg	0.33
B_S	2	D_P, m^{3}rad^{-1}	8×10^{-7}
Q_S	0.0002	K_S	1×10^7

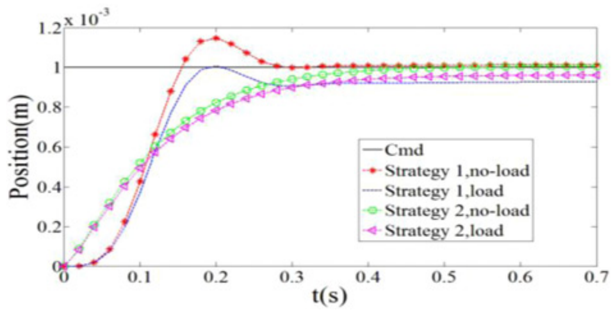

Fig. 6 *Position response to step command (X_C = 1 mm)*

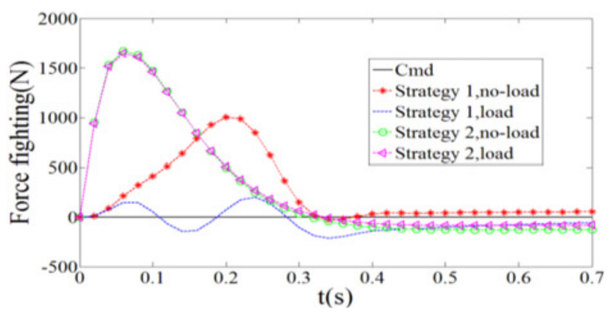

Fig. 7 *Force fighting to step command (X_C = 1 mm)*

only considers the positional parameter which owns a poor dynamic characteristic concerning the force fighting compensation. Meanwhile, it is also apparent that the processes of position response produce some overshoot under the control of strategy 1. The overshoot in the no-load state is more obvious, which reaches 15%.

As displayed in Fig. 7, the control strategy 1 is obviously better than the control strategy 2 in respect of the dynamic force fighting control efficiency. Under the control of strategy 2, the force fighting of the hybrid actuation in no-load state/load state are 1686 N/1655 N, respectively. However, they can be reduced to 998 N/202 N, respectively, under the control of strategy 1. This is because the velocity/position trade-off control strategy proposed in this paper not only considers the demand for control rod displacement, but also weighs the control requirement of piston velocity. Then, it can ensure the dynamic identical between two different types of actuators, thereby reducing the dynamic force fighting.

4 Operating model of HSA

4.1 Active/active mode

EHA and SHA adopt the position and velocity trade-off control strategy proposed in this paper, and the structure of the system is shown in Fig. 4. Step demand (1 mm position signal) is sent with external force at $t = 0$, then the simulation results are shown in Fig. 8.

As can be seen from Fig. 8, both actuators have nearly the same dynamic tracking ability, thereby HAS under this control strategy has little force fighting which has been verified in Section 3.4. Through Fig. 8, we can also get that the static position error for each actuator cylinder has narrowed almost to vanishing point. Therefore, when the system is stable, each actuator bears half of the entire load, respectively. However, the displacement of the control surface produces certain static error for the reason of spring quality factor.

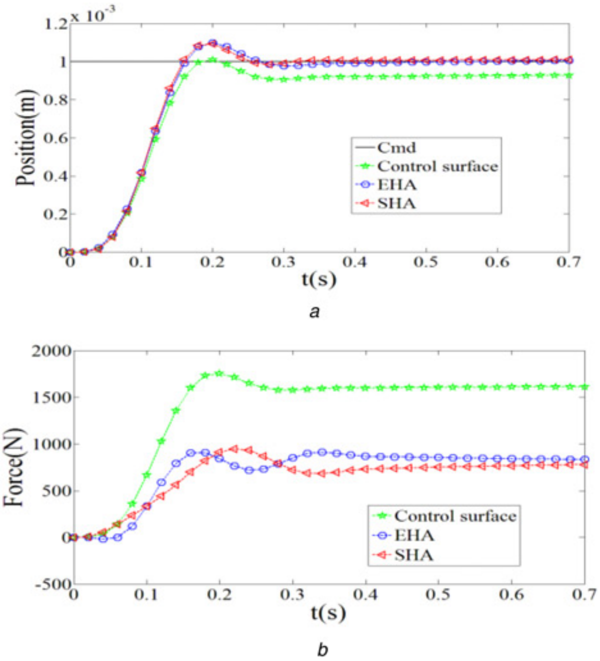

Fig. 8 *Dynamic responses in active/active mode by disturbance anticipation for a position step input ($X_C = 1$ mm, $t = 0$ s)*
a Position response
b Force response

4.2 Active/passive mode

In this mode, one actuator is actively controlled, and the other one is considered as the load following the motion of control surface. The schematic diagram of A/P mode is shown in Fig. 9.

Obviously, in this mode, no force fighting occurs. Based on the analysis in [2], the cavity of the hydraulic cylinder of the traditional SHA can be dredged via damping bypass valve to achieve a passive mode of operation. This working form can be applied to EHA as well. Therefore, there are two situations when the EHA/HAS HAS is operated in the A/P mode: one is that SHA is actively controlled, and EHA passively follows. The other one is that EHA is actively controlled, and SHA passively follows.

The simulation is carried out in the working condition in Section 4.1, and the simulation curves are available.

As can be seen from Fig. 10, due to following the movement of the control surface, the actuator in passive state generates a certain static error.

4.3 Operating mode switching analysis

Due to the breakdown of certain airborne equipment, the HAS would switch from active/active mode to A/P mode. In the active/active mode, each channel bears half of the air load. When a fault occurs, one of the channels is switched to passive mode, the other one is still in active mode which takes on the entire load.

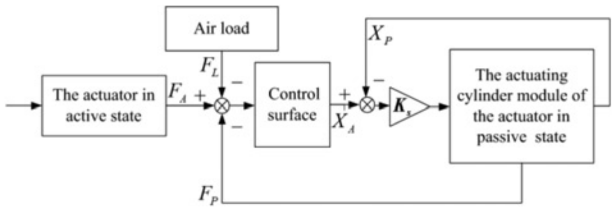

Fig. 9 *Principle diagram of A/P mode*

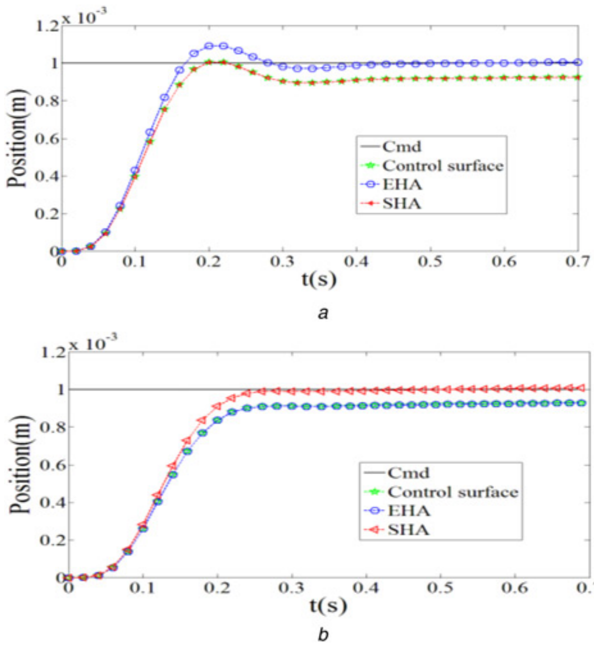

Fig. 10 *Position response in A/P mode by disturbance anticipation for a position step input ($X_C = 1$ mm, $t = 0$ s)*
a Position response when SHA is actively controlled
b Position response when EHA is actively controlled

During the whole process, the dynamic force of the system changes very violently, and it has a great impact on the system characteristics.

(i) Active/active mode switches to A/P mode in which the EHA is actively controlled throughout (the A/P mode 1).

Step demand (1 mm position signal) is sent at time 0 s with external force, and the hybrid actuator system is switched from active/active mode to A/P mode at $t = 1$ s. The EHA is in active state during the whole simulation process. The simulation results are shown in Fig. 11.

As can be seen from Fig. 11, when the HAS maintains in active/active mode, both actuators can response rapidly and synchronously under the control instructions, and the output force of each channel tends to be consistent at $t = 1$ s. When $t = 2$ s, the system operating mode is switched. SHA goes into the passive following state, so the EHA is gradually subjected to bear the entire aerodynamic load. It is observed that F_E increases from 788 to 1595 N. Correspondingly, F_S fells to 0 from 826 N. According to the analysis in Section 4.2, the closed-loop controller of SHA is no longer working when it is operated in passive state. Then the dynamic characteristics of SHA are completely determined by the motion of control surface. For this reason, the dynamic characteristics of the two working actuators are inconsistent. It is noted that F_S spends 0.06 s to reach the specified value, which is much faster than the reaction rate of EHA.

Meanwhile, it can be seen from Fig. 11*b* that the positions of both actuators are still basically kept in the instruction position. It shows that the hybrid actuator system can still meet the actuating requirements after switching from active/active mode to A/P mode.

Furthermore, when the system loads or unloads suddenly, the actuators generate a 180 Hz oscillation in the initial stage of the tracking process. This phenomenon is caused by the spring quality function, which is decided by attachment stiffness and load qualities.

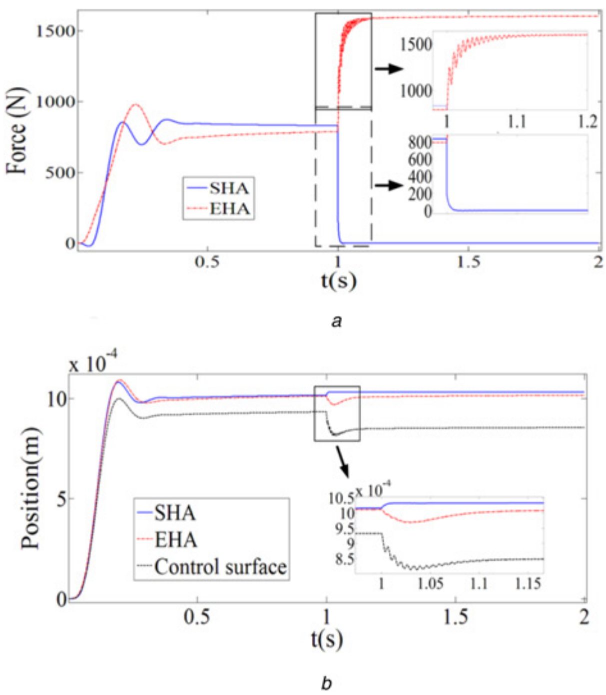

Fig. 11 *Dynamic characteristic of HAS during the mode switching process (EHA always maintains in active control state)*
a Output force of each actuator
b Position response of HAS

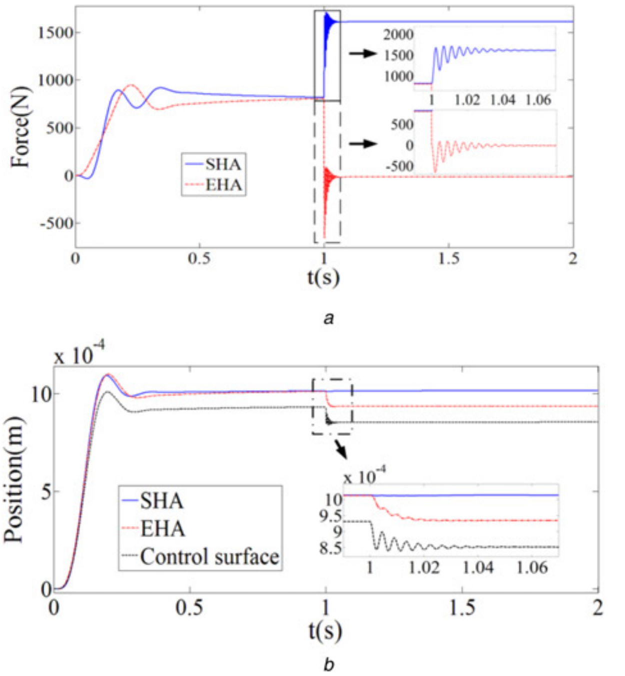

Fig. 12 *Dynamic characteristic of HAS during the mode switching process (SHA always maintains in active control state)*
a Output force of each actuator
b Position response of the HAS

(ii) Active/active mode switches to A/P mode in which the SHA is actively controlled throughout (the A/P mode 2).

Step demand (1 mm position signal) is sent at 0 s with external force, and the hybrid actuator system is switched from active/active mode to A/P mode at $t = 1$ s. In order to distinguish from the simulation which is mentioned in the previous paragraph, the SHA remains in the active control state throughout. The simulation results are shown in Fig. 12.

As displayed in Fig. 12, it can still meet the control requirements of the system in this operating mode. However, there still exist high-frequency oscillation in the operating mode switching process of the HAS. Compared with the A/P mode 1, the anti-disturbance performance of EHA is slightly worse than SHA's dynamic characteristic during the unloading process. However, the whole system can respond rapidly in the A/P mode 2.

5 Conclusion

Based on the elaboration of the working principle and system constitution of the hybrid redundant actuation system which is composed of EHA/SHA, a control strategy is proposed to compensate the dynamic force fighting by combining the trajectory generator with the weight coefficient theory. Subsequently, the mathematical modelling and simulation analysis are carried out as well. Finally, based on the above system, the dynamic characteristics of this system, switching from active/active mode to A/P mode, are analysed systematically. The following conclusions can be drawn.

(i) The position/velocity trade-off control strategy can significantly improve the dynamic characteristic control accuracy of HAS as long as it can ensure the static force fighting control effect. Meanwhile, the overall response time of HAS is greatly shortened by weighing the actuator velocity, which is a rapid response variable.

(ii) The actuator which is passively controlled in A/P mode would generate a static position error for the reason of pursuing the control surface movement.
(iii) After switching the operating mode from active/active to A/P mode, the performance of HAS can still meet the aircraft control requirements. However, no matter which channel is operated in the passive mode, the position of the control surface is reduced. In A/P mode 2, the HAS has better dynamic response characteristic during the process of switching.
(iv) Under the influence of spring quality factors which is decided by attachment stiffness and quality of control surface, the HAS produces a certain frequency oscillation under load disturbance. When the HAS switches to the A/P mode 2, this phenomenon is particularly acute.

6 References

[1] Bossche V.D.: 'Dominique. The 380 flight control electro-hydrostatic actuators, achievements and lessons learnt'. Proc. of the 25th Congress of the international Council of the Aeronautical Sciences, Hamburg, German, 2006

[2] Cochoy O., Hanke S., Carl U.B.: 'Concepts for position and load control for hybrid actuation in primary flight controls', *Aerosp. Sci. Technol.*, 2007, **11**, (2), pp. 194–201

[3] Fan D.L., Fu Y.L., Guo Y.Q., *et al.*: 'Dynamic force fighting for dissimilar redundant actuator syatem', *J. Beijing Univ. Aeronaut. Astronaut.*, 2015, **41**, (2), pp. 234–240

[4] Fu Y.L., Qi H.T., Wang L.J., *et al.*: 'Research on operating modes in hybrid actuation system', *Acta Aeronautica Et AstronauticaSinca*, 2010, **31**, (6), pp. 1178–1184

[5] Wang L.J., Mare J.C., Fu Y.L., *et al.*: 'Investigation in the dynamic force fighting of dissimilar redundant actuation systems operating in active/active mode'. 28th Int. Congress of the Aeronautical Sciences, Brisbane, Australia, 2012

[6] Fu Y.L., Fan D.L., Li Z.F.: 'Static force equalization for dissimilar redundant actuator system', *J. Beijing Univ. Aeronaut. Astronaut.*, 2014, **40**, (11), pp. 1492–1499

[7] Jacazio G., Gastaldi L.: 'Equalization techniques for dual redundant electro-hydraulic servo actuators for flight control systems'. Fluid Power and Motion Control, 2008

[8] Waheed U.R., Wang X.J., Wang S.P., *et al.*: 'Motion synchronization of HA/EHA system for a large civil aircraft by using adaptive control'. Proc. of 2016 IEEE Chinese Guidance, Navigation and Control Conf., Nanjing, China, 2016

[9] Waheed U.R., Wang S.P., Wang X.J.: 'A position synchronization control for HA/EHA system'. 2015 Int. Conf. on Fluid Power and Mechatronics, Harbin, China, 2015